INTERNATIONAL JOURNAL OF AGRICULTURE & BIOLOGY
ISSN Print: 1560–8530; ISSN Online: 1814–9596
19–1879/202x/00–0–000–000
DOI: 10.17957/IJAB/15.1443
http://www.fspublishers.org

Full Length Article

Chlorophyll *a* Fluorescence and Ginsenoside Content Reveal Photosystem II of *Panax quinquefolium* Responses to Two Seedbeds with Different Light Transmission Rates

Ying Lin[1,2], Lingna Wang[1], Shaoping Wang[2], Liming Li[3], Liming Sun[3], Yinglin Wang[4], Jingping Yu[4], Zhiping Qin[2], Heng Jiang[2], Jie Zhou[5], Jia Li[1] and Yongqing Zhang[1*]

[1]*School of Pharmacy, Shandong University of Traditional Chinese Medicine, Jinan, 250355, People's Republic of China*
[2]*School of Pharmacy, Binzhou Medical University, Yantai, 264003, People's Republic of China*
[3]*Wendeng Agricultural Bureau, Weihai, 264400, People's Republic of China*
[4]*College of Integrated Traditional Chinese and Western Medicine, Binzhou Medical University, Yantai, 264003, People's Republic of China*
[5]*School of Biological Science and Technology, University of Jinan, Jinan 250022, People's Republic of China*
[*]For Correspondence: zyq622003@126.com; linying_1980@163.com
Received 06 December 2019; Accepted28 February 2020; Published _____

Abstract

Cultivation of *Panax quinquefolium* L. (American ginseng) provides an alternative supply of this medicinal plant. Seedbeds are usually oriented east-west (E-W) or north-south (N-S). Because seedbeds are mounded rather than flat, the plants on either side are exposed to light with different incident angles. Therefore, we investigated the effect of the two seedbed orientations at different light transmission rates (LTRs) on photosystem II (PSII) through chlorophyll determination, gas exchange, the JIP-test, and ginsenoside analysis. Analysis of the kinetics of chlorophyll *a* fluorescence showed that the north side of the E-W bed at LTR of 20% (ES-20%) had the highest electron transfer rate and quantum yield, and a higher net photosynthesis (P_n). P_n and the concentrations of chlorophyll and ginsenosides increased with LTR. The other three positions had the highest Rg group ginsenoside contents (total content of ginsenosides Rg_1 and Re), which are an oxidative stress marker, indicating that photooxidation occurred, although the high P_n suggested that photoinhibition had not occurred. Thus, the PSII activity was highest for the ES-20% conditions, and the E-W seedbed with LTR of 20% had higher PSII activity and ginsenoside synthesis than the N-S seedbed. Moreover, the lowest P_n of the leaves obtained at LTR of 11% was attributed to the stomatal factor.

Key words: Seedbed; JIP-test; Light transmission rate; *Panax quinquefolium*; Photosynthesis

Introduction

Panacis quinquefolii radix is an important traditional Chinese medicine that comes from the dried root of *Panax quinquefolium* L. (American ginseng); a plant that belongs to the Araliaceae family (Rao *et al*. 2004; Proctor *et al*. 2010; Chinese Pharmacopoeia Commission 2015). Ginsenosides, which are secondary metabolites of American ginseng, possess diverse pharmacological activities, which include stimulating cell metabolism, enhancing immune system function, protecting the cardiovascular system, and antioxidant and anticancer properties (Attele *et al*. 1999; Liao *et al*. 2002; Xie *et al*. 2007; Yuan *et al*. 2010; Qi *et al*. 2011; Kim 2012; Wang *et al*. 2013; Kochan *et al*. 2014; Shkryl *et al*. 2018). Ginsenosides are classified into the following three groups according to their structures: protopanaxadiols (Rb group: Ra_1, Ra_2, Rb_1, Rb_2, Rb_3, Rc, Rd, Rg_3, Rh_2, and others); protopanaxatriols (Rg group: Rg_1, Rg_2, Re, Rf, Rh_1, and others); and oleanolic acid derivatives (Ro group: oleanolic acid) (Wang *et al*. 2013; Kochan *et al*. 2014).

American ginseng is at risk of extinction because of threats to its natural habitat and overexploitation (Shkryl *et al*. 2018). Hence, wild resources are rare and cannot satisfy growing medicinal demand. Cultivation is an alternative way to supply this plant with high medicinal substances (Wang and Wu 2003; Proctor *et al*. 2010). In China, American ginseng is cultivated at 25 cm high and 1.5 m wide seedbeds (Hou 2017), whereas the length and direction are determined by the situation of the cultivated land. Therefore, the long axis of the seedbeds can be oriented east-west (E-W) or north-south (N-S). Because the seedbeds are not strictly flat, the short-axis section is slightly mounded. Thus, the leaves of American ginseng

To cite this paper: Lin Y, L Wang, S Wang, L Li, L Sun, Y Wang, J Yu, Z Qin, H Jiang, J Zhou, J Li, Y Zhang (202x). Chlorophyll *a* fluorescence and ginsenoside content reveal photosystem II of *Panax quinquefolium* responses to two seedbeds with different light transmission rates. *Intl J Agric Biol* 00:000–000

growing on different sides of the seedbeds have different orientations. Studies on other plants have shown that the ridge direction alters the light intensity that reaches the leaves, and thus affects the photosynthesis and yield of plants (Ma *et al*. 2015).

American ginseng is a shade perennial, and its growth and development are sensitive to light intensity (Proctor *et al*. 2010; Cheng and Shen 2011; Proctor and Palmer 2017). Lower light intensity cannot maintain the normal level of photosynthesis and reduces the yield, whereas higher light intensity bleaches the leaves, inhibits photosynthesis, and causes severe death of leaves and plants (Proctor and Palmer 2017). The optimum light intensity for American ginseng is determined by age. Generally, the appropriate range of light transmission rate (LTR) of 1 to two-year-old plants is 18–20%, whereas for 3 to four-year-old plants, it is 25–30% (Li *et al*. 2004; Wang *et al*. 2010). Therefore, it is essential to provide optimum light intensity for American ginseng during cultivation.

Methods for studying plant photosynthesis include determination of leaf gas exchange parameters and fast chlorophyll *a* fluorescence induction kinetics. Fast chlorophyll *a* fluorescence analysis is a transient record of a plant or leaf or photosynthesizing organism exposed to actinic radiation 1–2 s. This transient record has a typical polyphasic O-J-I-P (OJIP curve) shape. O refers to the initial fluorescence level at 20 μs; J and I refer to the fluorescence level at 2, 3 and 30 ms, respectively; and P refers to the maximum fluorescence level (Gao *et al*. 2018). Thus, fast chlorophyll *a* fluorescence analysis is also called the JIP-test (Campos *et al*. 2014; Yang *et al*. 2018). The JIP-test provides information about the structure, activities, and electron transport of PS Ⅱ. The method has the advantages of measuring more than 50 parameters, being fast (1–2 s), and not damaging the plants. Although the JIP-test is widely used to study plant photosynthesis (Li *et al*. 2006; Cuchiara *et al*. 2013; Jedmowski *et al*. 2015), there are few reports on the photosynthesis of American ginseng.

We hypothesize that the growing position and LTR could affect the activities of PSII in American ginseng. Therefore, we examined the photosynthesis, chlorophyll concentration, OJIP curve, parameters related to the JIP-test, and the ginsenoside contents of two-year-old American ginseng grown on different sides of seedbeds with N-S or E-W orientations and different LTRs.

Materials and Methods

Plant material and growth conditions

The plants were grown in an experimental field of Wendeng Agricultural Bureau, Wendeng, Shandong Province, China (37°12′N, 122°03′E). Wendeng is located in the North Temperate Zone and has a continental monsoon climate. The average annual temperature is 11.1ºC. The annual precipitation is 816.7 mm, which mainly occurs in summer, accounting for 82.2% of the total rainfall amount, whereas there is less precipitation in spring and autumn, and drought often occurs in these two seasons. The annual sunshine is 2522 h and the frost-free period is 194 days.

The study was carried out from March 16 to October 16, 2018. Six shading sheds (area of 50 m^2 each and height of 1.8 m) were constructed, and the LTRs of the sheds were 11, 15, and 20%. There were two sheds for each LTR, one containing N-S seedbed and the other containing an E-W seedbed. The LTR in each experiment was controlled by the number of layers of black polyethylene net. The conditions in which the plants were cultivated were named according to the orientation and side of the seedbed and the LTR (Table 1). For example, the south side of the E-W seedbed with LTR of 15% is called ES-15%.

Two-year-old American ginseng plants were obtained from Wendeng Agricultural Bureau, and were transplanted into the seedbeds (length × width × height, 10 × 1.5 × 0.25 m) at a density of 1 plant per 20 × 8 cm on March 16, 2018 (Hou 2017). The seedbed soil had a pH of 4.69, hydrolyzed nitrogen of 52.9 $mg \cdot kg^{-1}$, available phosphorus of 140.9 $mg \cdot kg^{-1}$, available potassium of 65 $mg \cdot kg^{-1}$, and organic matter of 1.03%. The field management measures of each treatment were consistent.

Measurements of gas exchange parameters

The net photosynthesis rates (P_n), stomatal conductance (g_s), and internal CO_2 (C_i) of the fully expanded two-year-old American ginseng leaves were determined by a portable photosynthesis system (CIRAS-3, PP Systems, Amesbury, MA, USA). Measurements were taken during the period of fastest root growth (Liu *et al*. 1987), at 09:00–11:00 am on August 10, 2018 on a sunny day under light saturation (700 $\mu mol \cdot m^{-2} \cdot s^{-1}$), illumination, ambient carbon dioxide of 400 ppm, average, relative humidity of 40%, and temperature of 30ºC.

Determination of chlorophyll content

The chlorophyll contents of two-year-old American ginseng leaves were measured with a chlorophyll meter (SPAD-502, Minolta, Tokyo, Japan) at the center of the full expanded leaves, except for major veins.

JIP-test

Fast chlorophyll *a* fluorescence transient tests of the fully expanded leaves of two-year-old American ginseng were performed from 09:00 to 11:00 am on a sunny day using a Plant Efficiency Analyzer (Handy PEA, Hansatech Instruments Ltd., UK). After 30 min dark adaptation using dark adaptation clips on the leaves, as described previously (Li *et al*. 2006), the middle leaflet was illuminated with continuous red light (peak at 650 nm) for 1 s at 3000 $\mu mol \cdot m^{-2} \cdot s^{-1}$ to generate a true maximum fluorescence

Table 1: Summary of conditions during the course of experiment

Group name	Conditions
ES-11%, ES-15%, ES-20%	South side of the E-W seedbed, LTRs of 11%, 15%, and 20%, respectively.
EN-11%, EN-15%, EN-20%	North side of the E-W seedbed, LTRs of 11%, 15%, and 20%, respectively.
NE-11%, NE-15%, NE-20%	East side of the N-S seedbed, LTRs of 11%, 15%, and 20%, respectively.
NW-11%, NW-15%, NW-20%	West side of the N-S seedbed, LTRs of 11%, 15%, and 20%, respectively.
N-11%	Both sides of the N-S seedbed, LTR of 11% (i.e., NE-11% and NW-11%)
N-15%	Both sides of N-S the seedbed, LTR of 15% (i.e., NE-15% and NW-15%)
N-20%	Both sides of N-S the seedbed, LTR of 20% (i.e., NE-20% and NW-20%)
E-11%	Both sides of E-W the seedbed, LTR of 11% (i.e., ES-11% and EN-11%)
E-15%	Both sides of E-W the seedbed, LTR of 15% (i.e., ES-15% and EN-15%)
E-20%	Both sides of E-W the seedbed, LTR of 20% (i.e., ES-20% and EN-20%)

intensity (Ma *et al*. 2017).

The OJIP curve was obtained from the fast chlorophyll *a* fluorescence transient test. The meanings and analysis methods of each parameter and the phases of the OJIP curve are described in the literature (Strasser *et al*. 2000; Force *et al*. 2003; Strasser *et al*. 2004; Li *et al*. 2006; Stirbet and Govindjee 2011) and methods of normalization of the initial curve acquired from the JIP-test have been described previously (Qiu *et al*. 2012). In this study, the two methods of normalization were as follows. First is normalization with $(F_M - F_0)$, where the normalized fluorescence signal data is relative variable fluorescence, $V_t = (F_t - F_0)/(F_M - F_0)$, and F_t is the fluorescence value at time *t*, F_M is the maximum fluorescence, and F_0 is the initial fluorescence. In the OJIP curve plotted with V_t, the value of the O-phase is 0, whereas that of the P-phase is 1. The second is normalization with $(F_J - F_0)$, where the normalized fluorescence signal data is $W_t = (F_t - F_0)/(F_J - F_0)$, and F_J is the fluorescence at the J-step. In the OJIP curve plotted with W_t, the value of the O-phase is 0, whereas that of the J-phase is 1.

Fluorescence parameters can be obtained by mathematical analysis of the fluorescence kinetic curve (Strasser *et al*. 2000; Strasser *et al*. 2004). In this study, the radar plot was constructed from the fluorescence parameters obtained for the NW-15% conditions with a calculated value of 1, and the ratio of the fluorescence parameters obtained for the other conditions to the control parameters.

High-performance liquid chromatography analysis of ginsenosides

The roots of the 12 groups of plants were collected on October 16, 2018. The roots were washed sequentially with clean water and distilled water, and then the residual water was removed with absorbent paper. The cleaned roots were cut into slices 1 cm thick, kept initially at 38ºC for 24 h, and then at 40ºC until dried.

For each group of plants, 1 g dried powder from 20 dried American ginseng plants was placed in a conical flask with a plug, extracted with 50 mL of water-saturated *n*-butanol by refluxing for 1 h, cooled to room temperature, and filtered. A 10 mL sample of the extracted solution was evaporated to dryness. The residue was dissolved in 50% methanol, and adjusted to an exact volume of 5 mL using a 5 mL volumetric flask. The extract was filtered through a membrane filter with a pore size of 0.45 μm. The filtrate was used for high-performance liquid chromatography (HPLC) analysis (Yu *et al*. 2019).

Standard ginsenoside components, such as ginsenosides Rg_1, Re, Rb_1, Rc, and Rd, were purchased from Shanghai Yuanye Bio-Technology Co., Ltd. (Shanghai, China). The HPLC separation was carried out on an HPLC system (U3000, Thermo Fisher Scientific, Waltham, MA, USA) with a C18 column (4.6 × 250 mm, 5 μm), at a temperature of 40ºC, a flow rate of 1 mL·min^{-1}, and a detection wavelength of 203 nm. The mobile phases were acetonitrile (Solvent A) and 0.05% phosphoric acid (Solvent B) and the gradient was as follows: 19% A (0–35 min); 19–29% A (35–70 min); 29–40% A (70–100 min). A one-point curve method was used for ginsenoside quantification analysis (mg·g^{-1} DW) and was performed by comparing retention times and peak areas of standards and samples (Yu *et al*. 2019). The total content of Rg_1 and Re is the Rg group content, the total content of Rb_1, Rc, and Rd is the Rb group content, and the ratio of the two values is Rg/Rb (Jang *et al*. 2015).

Statistical analysis

All measurements were repeated six times. All statistical analyses were performed by using SAS 19.0 software (SAS Institute, Cary, NC, USA). The statistical significance of the differences was determined using Duncan's multiple range test and one-way analysis of variance (ANOVA), evaluating significant differences at $P < 0.05$. All data were compared at the 5% significance level and were reported as mean ± standard deviation.

Results

Effects of LTRs and seedbed orientation on P_n, g_s, and C_i

In seedbeds with the same orientation, P_n and g_s of American ginseng leaves grown on both sides of the seedbeds increased with LTR significantly ($P < 0.05$) (Fig. 1). At the same LTR, P_n and g_s showed no significant difference between the two sides of the same seedbed ($P > 0.05$), except for the E-11% conditions ($P < 0.05$), for which

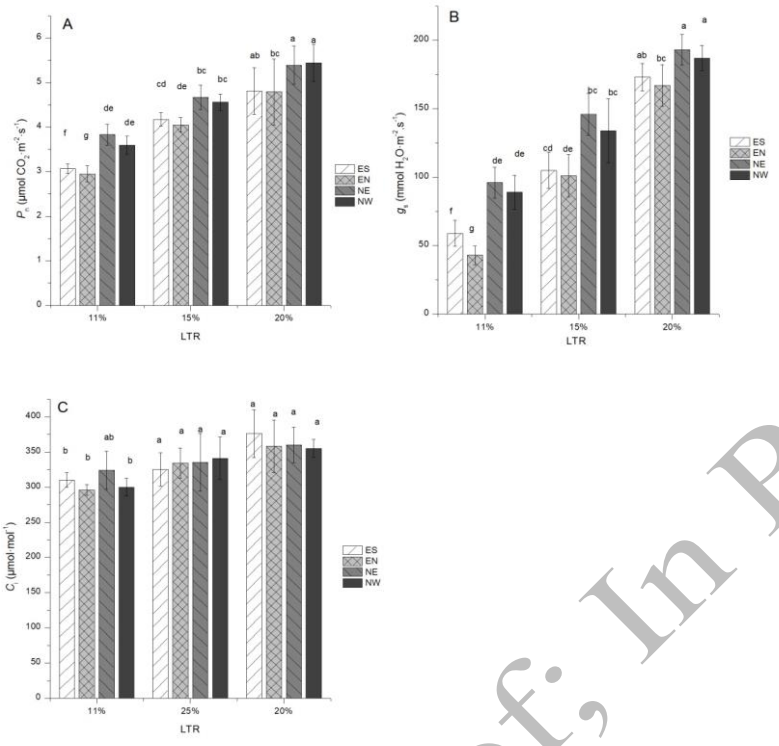

Fig. 1: P_n (A), g_s (B), and C_i (C) of 2-yr-old American ginseng grown on two seedbeds with different LTRs
The vertical error bars represent the standard errors ($n = 6$). The same letters at the top of each bar indicate that there is statistically no difference at $P > 0.05$ using Duncan's multiple range test

the values of P_n and g_s were the lowest. However, this difference was not observed for the N-11% conditions. Otherwise, at the same LTRs, the parameters for the leaves grown on both sides of the E-W seedbeds were lower than those for the N-S seedbeds ($P < 0.05$). C_i was the same for LTRs of 20% and 15% ($P > 0.05$) (Fig. 1). C_i values for LTR of 11%, except for the NE-11% conditions, were the smallest compared with those for LTRs of 20% and 15% ($P > 0.05$), and the NE-11% conditions showed no differences from those with LTRs of 20% and 15% ($P > 0.05$).

Effects of LTRs and seedbed orientation on chlorophyll content

On the south side of the E-W seedbeds, the chlorophyll content of the American ginseng leaves increased with increase in LTR; ES-11% had a significantly lower content than ES-15% and ES-20% ($P < 0.05$), although there was no significant difference between ES-15% and ES-20% (Fig. 2). On the north side of the E-W seedbeds, the same trend was observed, and significant differences were observed ($P > 0.05$) among the three LTRs (EN-11%, EN-15%, and EN-20%). Otherwise, there were no significant differences between the sides of the N-S seedbeds for the three LTRS ($P > 0.05$).

At LTR of 11%, the chlorophyll content for both sides of the N-S seedbeds were significantly higher than those for the E-W seedbeds ($P < 0.05$), whereas the content was similar for both sides of seedbeds with the same orientation ($P > 0.05$). For LTRs of 15%, NW-15% had the highest content, followed by NE-15%, ES-15%, and EN-15%. EN-15% was the lowest, and showed a significant ($P < 0.05$) difference from NW-15% and NE-15%. ES-15% was higher than EN-15% ($P > 0.05$), and lower than NW-15% ($P < 0.05$) and NE-15% ($P > 0.05$). The chlorophyll contents for groups with LTR of 20% were greater than those of the other LTRs, and there were no differences among the groups with LTR of 20% ($P > 0.05$).

Effects of LTRs and seedbed orientation on chlorophyll *a* fluorescence transients

Chlorophyll *a* fluorescence is a sensitive method for studying the performance of PSII. OJIP-curves normalized by V_t and W_t of American ginseng grown in seedbeds with two different orientations and different LTRs are shown in Fig. 3A–B. The OJIP chlorophyll *a* fluorescence-induced kinetics curves were typical, indicating that the plants had a normal status. The fluorescence intensity of the J-step of EN-11% was the biggest, followed by ES-11%, and the values for the other groups were similar (Fig. 3A). The fluorescence intensity of the I-step of EN-11% was the largest, followed by NW-20% and NE-11%, and the values for NE-20% and ES-20% showed a dramatic decrease (Fig. 3B). For the P-step, the fluorescence intensity of EN-11% was the biggest, whereas the values for NE-20% and ES-

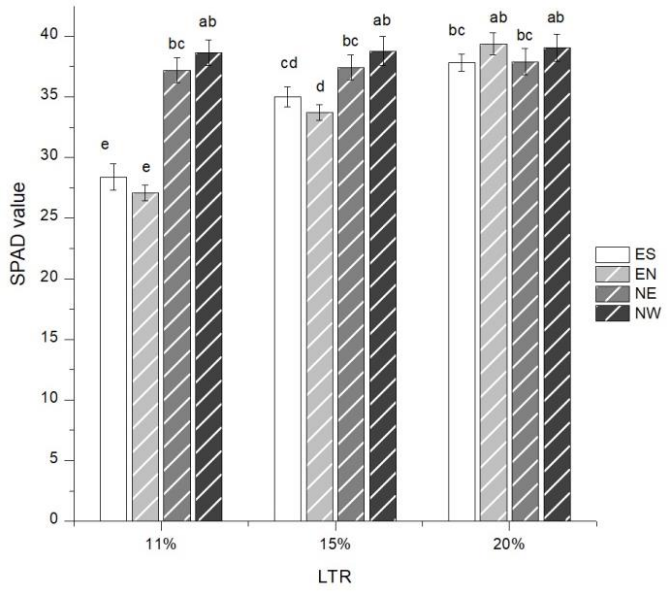

Fig. 2: Chlorophyll contents of 2-yr-old American ginseng grown on two seedbeds with different LTRs
The vertical error bars represent the standard errors (n = 6). The same letters at the top of each bar indicate that there is statistically no difference at $P > 0.05$ using Duncan's multiple range test

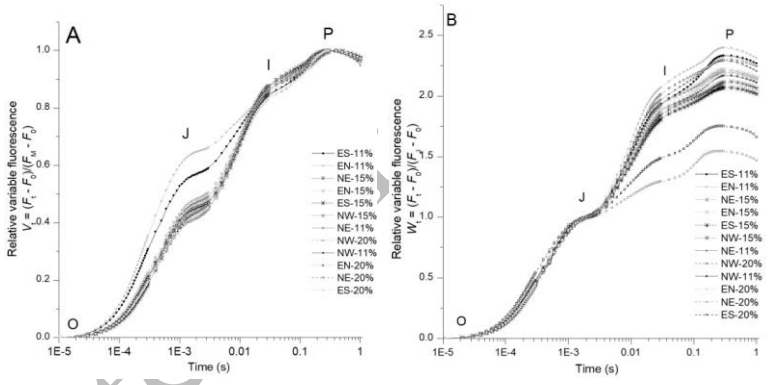

Fig. 3: Fast chlorophyll fluorescence curves normalized by V_t (A) and W_t (B) (n = 6)

20% were the lowest, the same as for the I-step (Fig. 3B).

The heterogeneity of the oxidized plastoquinone (PQ) pool is reflected by phases J-I and I-P. The PQ pool can be divided into the rapidly reducible PQ pool (phase J-I) and slowly reducible PQ pool (phase I-P). In the J-I phase, the fluorescence intensity of EN-11% was the highest, whereas that of NE-20% was the lowest ($P < 0.05$) (Fig. 3A). The I-P phase was the same as the J-I phase, although the fluorescence intensities of NE-20% and ES-20% were the lowest ($P < 0.05$) (Fig. 3B). Both the rapidly and slowly reducible PQ pools of the leaves in the NE-20% and ES-20% groups were the largest, whereas those in the EN-11% group were the smallest.

In this study, the seven fluorescence parameters with the most fundamental physiological significance are shown in Table 2 and Fig. 4. The maximum quantum yields for PSII photochemistry, F_V/F_M, were the lowest for EN-11% and ES-11% ($P < 0.05$), and there was no significant ($P > 0.05$) difference between them (Table 2, Fig. 4). The largest values of F_V/F_M were recorded for ES-15% and ES-20%, and these values showed significant differences to the other groups ($P < 0.05$), although there was no significant difference between them ($P > 0.05$). In the E-W seedbeds, F_V/F_M values for plants grown on the south side of the seedbed with the same LTR were larger than those grown on the north side, and there were significant differences ($P < 0.05$) between the two sides of the seedbeds for LTRs of 15 and 20% (E-15% and E-20%). In contrast, there was no significant ($P > 0.05$) difference in values between the two sides of the E-W seedbed with an LTR of 11% (E-11%). There was no difference ($P > 0.05$) between the sides of the N-S seedbeds for the three LTRs (N-11%, N-15%, and N-20%). The values of F_V/F_M for E-11% were the lowest, whereas those

Table 2: Parameters of JIP-test in dark-adapted leaves

LTR	Fv/F_M	V_J	V_I	S_m	N	RC/CS_m	PI total
NW-20%	0.7900±0.017b	0.5254±0.008d	0.8823±0.006f	17.8733±0.009j	28.5156±0.568m	1671.81±134.227q	0.4637±0.029t
NE-20%	0.7934±0.021b	0.5038±0.003d	0.8802±0.002f	18.4434±2.114i	30.2525±1.266l	1694.6034±114.552q	0.5353±0.009t
ES-20%	0.8052±0.002a	0.4658±0.017e	0.8632±0.046g	23.0241±2.444h	36.3403±0.954K	3552.5556±150.553n	0.9100±0.065r
EN-20%	0.7951±0.003b	0.4719±0.009e	0.8714±0.044g	20.0975±0.521i	33.6774±0.649l	3451.6111±89.774p	0.9849±0.054r
NW-15%	0.7873±0.003b	0.462±0.013e	0.8455±0.010g	22.0076±3.663h	35.5831±0.756k	3352.2727±44.228p	0.7815±0.128s
NE-15%	0.7767±0.012b	0.4386±0.004e	0.8325±0.004g	23.6752±3.591h	36.9804±1.031k	3107.8571±164.014p	0.6437±0.110s
ES-15%	0.7994±0.002a	0.4285±0.017e	0.866±0.014g	19.5791±1.031i	32.7989±1.276l	3284.625±147.222p	0.7229±0.134s
EN-15%	0.7956±0.024b	0.4497±0.015e	0.8625±0.041g	18.8403±2.131i	31.3094±1.243l	3237.8182±123.996p	0.6852±0.017s
NW-11%	0.7866±0.003b	0.4930±0.007d	0.8766±0.005f	18.3296±1.423i	29.5854±2.475l	3439.0556±112.669p	0.8642±0.064s
NE-11%	0.7991±0.005b	0.4886±0.006d	0.8750±0.046f	19.6168±0.475i	30.6032±0.753l	3383.8889±130.653p	0.7825±0.048s
ES-11%	0.743±0.004c	0.5800±0.013d	0.8501±0.006g	26.5799±1.354h	46.5620±9.765k	3043.0000±109.271p	0.5700±0.050s
EN-11%	0.7197±0.001c	0.6593±0.054d	0.8438±0.002g	17.9446±0.429i	33.8413±5.629k	3092.0909±115.207p	0.5873±0.040s

Mean values ± standard error based on six independent determinations. The same letters at the end of each value indicate that there is statistically no difference at $P > 0.05$ using Duncan's multiple range test

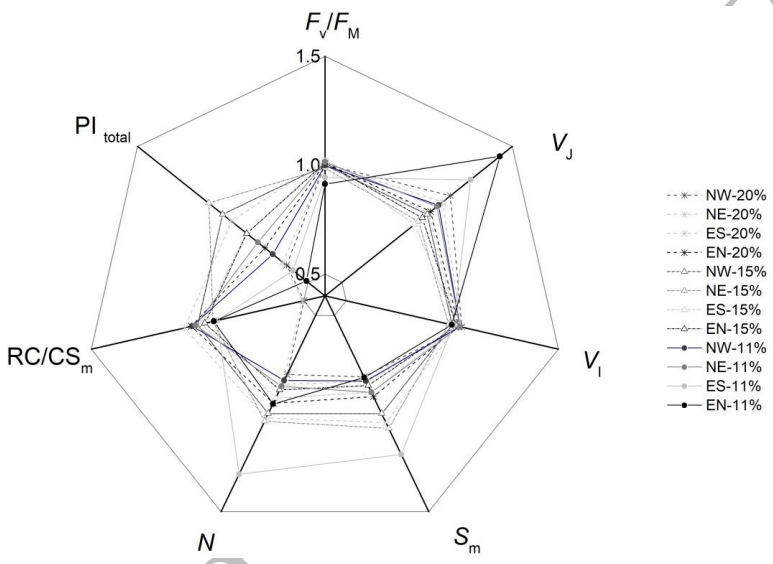

Fig. 4: Radar plot of parameters derived from the JIP-test

Measurements were carried out in dark adapted leaves of the plants. Average values are expressed in relation to the plants under SW-15% conditions, for which the values were normalized to 1. Data are mean values ($n = 6$)

for ES-20% were the highest.

The 12 groups of plants were divided into two groups according to the significance of the relative variable fluorescence at 2 ms, V_J, and the relative variable fluorescence at 30 ms, V_I (Table 2; Fig. 4). For V_J, N-20% and the conditions with LTR of 11% (N-11% and E-11%) were in the higher V_J group, whereas the other conditions were in the lower V_J group, and the V_J values of the two groups were significantly different from each other ($P < 0.05$). For V_I, N-11% and N-20% were in the higher V_I group, whereas the other conditions were in the lower V_I group, and there was a significant difference between the two groups ($P < 0.05$).

The conditions were divided into three groups according to the significance ($P < 0.05$) of total electron carriers per reaction center (RC), S_m, and time-dependent turnover number of primary quinone electron acceptor of PSII (Q_A), N (Table 2; Fig. 4). ES-20%, N-15%, and ES-11% had the highest S_m values, the value of NW-20% was the lowest ($P < 0.05$), and the values of the other six conditions were intermediate. The values of N were similar to those of S_m, except that the group with the highest values consisted of ES-20%, E-11%, and N-15%, and the other conditions had similar values.

The value of RC/CS_M [number of active PSII reaction centers per unit area ($t = t_{FM}$)] and PI_{total} [performance index (potential) for energy conservation from photons absorbed by PSII to the reduction of PSI end acceptors] for N-20% was the lowest (Table 2, Fig. 4). The value of RC/CS_M for ES-20% was the biggest, and the value of PI_{total} for EN-20% and ES-20% were the biggest ($P < 0.05$).

Effects of LTRs and seedbed orientation on ginsenoside contents

The ginsenoside contents of Rg_1, Re, Rb_1, Rc, and Rd are shown in Table 3. For the same LTRs, the contents of Re, Rb_1, and Rc decreased in the order of seedbed orientation

Table 3: Ginsenoside composition in roots

LTR	Rg_1	Re	Rb_1	Rc	Rd
NW-20%	0.4392±0.0685b	5.7303±0.5432d	9.0580±1.4553g	9.1476±0.9933m	1.1353±0.3590x
NE-20%	0.4370±0.0543b	5.6149±0.7765d	9.0394±1.5642g	9.1175±0.9694m	1.1275±0.6543x
ES-20%	0.4364±0.0323b	5.5081±0.8392d	8.9873±1.7653g	8.9536±0.8833m	1.1620±0.3345x
EN-20%	0.4132±0.0453c	5.3420±0.8372e	8.9566±1.4421h	8.6098±1.1124n	1.6788±0.3821w
NW-15%	0.4012±0.0654c	5.3002±0.5564e	8.8397±1.2212h	8.5893±1.0235n	1.7345±0.5467w
NE-15%	0.4555±0.0699b	5.2260±0.0222e	8.7847±1.3424h	8.5672±0.8839n	1.6717±0.4321w
ES-15%	0.4373±0.0943b	5.2020±0.0543e	8.7768±1.6537h	8.5691±0.6623n	1.6596±0.2231w
EN-15%	0.4243±0.0754b	5.2254±0.0768e	8.8781±1.8724h	8.5848±0.7653n	1.7082±0.3234w
NW-11%	0.4620±0.1094a	4.6141±0.0599f	7.6815±1.5541k	7.6241±0.9782p	1.6134±0.6998w
NE-11%	0.4636±0.0884a	4.5067±0.4998f	7.6376±1.6241k	7.1050±0.6136p	1.1980±0.7742x
ES-11%	0.4558±0.0675a	4.1868±0.0740f	7.2704±1.2342k	6.9075±0.1100p	0.9237±0.2211y
EN-11%	0.4523±0.0433a	4.1831±0.0042f	7.2463±1.4456k	6.8856±0.3345p	0.9170±0.1021y

Mean values ± standard error based on six independent determinations. The same letters at the end of each value indicate that there is statistically no difference at $P > 0.05$ using Duncan's multiple range test

and side of NW, NE, ES, and EN, except for Rb_1 and Rc for EN-15%, although there were no significant differences ($P > 0.05$). Maximum Re, Rb_1, and Rc contents were observed for the N-20% and ES-20% conditions, and showed significant differences compared with the other conditions ($P < 0.05$). Re, Rb_1, and Rc contents for LTR of 11% for both orientations (N-11% and E-11%) were significantly lower than those for other conditions ($P < 0.05$), but there was no difference among the contents for N-11% and E-11% ($P > 0.05$).

The contents of Rg_1 for LTR of 11% (N-11% and E-11%) were higher than those for the other LTRs ($P < 0.05$). For LTR of 20%, the Rg_1 contents of the roots of the plants grown on both sides of the N-S seedbeds (N-20%) were higher than those of the E-W seedbeds (E-20%). For LTR of 15%, the Rg_1 content of NW-15% was the lowest, and showed a significant difference from the other three groups with the same LTR ($P < 0.05$) (Table 3).

The Rd content increased, and then decreased as the LTR increased (Table 3). The conditions were divided into three groups according to their significance ($P < 0.05$). The group with the highest Rd contents consisted of EN-20%, E-15%, N-15% and NW-11% ($P < 0.05$), and there were no significant differences among the members of this group ($P > 0.05$). N-20%, ES-20%, and NE-11% had the second highest Rd contents, and there was no significant difference among the group ($P > 0.05$). E-11% had the lowest Rd, and there was no significant difference between the two sides of the seedbed ($P > 0.05$).

The total concentrations of the Rg and Rb groups and the Rg/Rb indices are shown in Table 4. The values of the Rg groups for NE-20%, NW-20%, and ES-20% showed no significant differences ($P > 0.05$), and were significantly higher than the values for the other groups ($P < 0.05$). ES-11% and EN-11% had the lowest values that were significantly ($P < 0.05$) lower than those for the other groups, although there was no significant ($P > 0.05$) difference between these two groups. These values for the Rb groups followed a similar trend to the values for Rb_1. The values of Rb groups for NW-20%, NE-20%, and ES-20% were significantly ($P < 0.05$) higher than those for the other groups, whereas those for E-11% and N-11% differences were the lowest ($P < 0.05$).

NW-20% had the highest Rg/Rb ratio, with 1.08-fold more ginsenosides than EN-15%, which had the lowest ratio ($P < 0.05$). The ratios for LTR of 11% were not the lowest, and were close to those for ES-20% ($P > 0.05$). A total of five ginsenosides were significantly up-regulated as the LTRs increased markedly ($P < 0.05$), which was consistent with the trend for P_n (Fig. 1A).

Discussion

Photosynthesis is the basis of plant morphogenesis, growth, and development. Because photosynthesis provides 90–95% of the plant's dry weight, it is crucial to the quality and yield of the plant (Cheng and Shen 2011). Light transmission and the planting position affects the effective light intensity on leaves, especially for shade plants like American ginseng (Wang *et al*. 2010; Xu *et al*. 2011; Li *et al*. 2014; Song *et al*. 2017).

We investigated the response of PSII in two-year-old *P. quinquefolium* plants to different LTRs and seedbed orientations through gas exchange, JIP-test, chlorophyll content determination, and ginsenoside analysis. The seedbed orientation seemed to have no effect on the chlorophyll content below LTR of 20%, and increasing the LTR increased the chlorophyll content of the leaves of *P. quinquefolium*.

The quantum yields (F_V/F_M) indicated that conditions E-11% (ES-11% and EN-11%) and ES-20% had the largest and smallest effects on the light photochemical efficiencies of the leaves, respectively (Li *et al*. 2006). The J-step (the fluorescence intensity at 2 ms) corresponds to the first transient accumulation of the primary quinone electron acceptor of PSII (Q_A), and reflects the efficiency of the electron transfer and the degree of closure of active RCs (Force *et al*. 2003; Li *et al*. 2006). When the LTR was 11%, 2 ms after illumination, the electron reception on the acceptor side of PSII (J-step) and the proportions of RCs were smallest for the plants grown under E-11% conditions (Li *et al*. 2006). That is, on the acceptor PSII side, the transport of electrons from Q_A^- to the secondary acceptor Q_B was blocked, and the majority of the active RCs were shut

Table 4: Total concentration of Rg and Rb groups and Rg/Rb index in roots

LTR	Rg	Rb	Rg/Rb	Total
NW-20%	6.1695±0.9933a	19.3410±1.5632d	0.3190±0.0112g	25.5105±1.5412k
NE-20%	6.0520±0.8970a	19.2844±2.0013d	0.3138±0.0287g	25.3363±4.2210k
ES-20%	5.9445±0.9782a	19.1029±1.0093d	0.3112±0.0491g	25.0474±2.1240k
EN-20%	5.7552±0.9932b	19.2452±1.1209e	0.2990±0.0352i	25.0004±2.6786m
NW-15%	5.7014±0.6352b	19.1635±1.4325e	0.2975±0.0333i	24.8649±1.4432m
NE-15%	5.6815±0.8897b	19.0236±1.6320e	0.2987±0.0549i	24.7051±1.0098m
ES-15%	5.6394±0.6722b	19.0054±1.4424e	0.2967±0.0093i	24.6448±1.7849m
EN-15%	5.6497±0.5409b	19.1711±1.6521e	0.2947±0.2019i	24.8208±1.3030m
NW-11%	5.0761±0.2095b	16.9190±1.7732f	0.3000±0.1129h	21.9951±1.3950n
NE-11%	4.9704±0.1443b	15.9406±1.5430f	0.3118±0.0388h	20.9110±1.3306n
ES-11%	4.6425±0.3320c	15.1016±1.4352f	0.3074±0.0408h	19.7441±1.4509n
EN-11%	4.6354±0.4234c	15.0488±1.6642f	0.3080±0.0333h	19.6842±1.8876n

$Rg = Rg_1 + Re$; $Rb = Rb_1 + Rc + Rd$. Mean values ± standard error based on six independent determinations. The same letters at the end of each value indicate that there is statistically no difference at $P > 0.05$ using Duncan's multiple range test

down (Bordenave *et al*. 2019). Thus, electrons could not be transferred to the dark reactions (Pan *et al*. 2010), which down-regulated the assimilatory power and the rate of the dark reaction during carbon assimilation and reduced the production of photosynthates (Sun *et al*. 2009).

For LTR of 20%, the values of P_n for N-20% and ES-20% were the largest. For ES-20%, the value of the maximum quantum yield of PSII (F_V/F_M), performance indexes (PI_{total}), and number of active PSII (Q_A reducing) RCs per unit area (RC/CS_M, $t = t_{FM}$) were the highest (Li *et al*. 2006). A highest rapidly reducible PQ pool (J-I phase) and slowly reducible PQ pool (I-P phase) together resulted in the highest time-dependent turnover number of Q_A (N), most electron carriers per RC (S_M), and the lower proportions of reaction centers (RCs) closed at 2 ms (V_J) and 30 ms (V_I). A higher chlorophyll content of ES-20% also prompted the electron transfer rate and the quantum yield of electron transport beyond Q_A (Li *et al*. 2006; Qiu *et al*. 2012). In addition, total electron carriers per RC (S_m) and time-dependent turnover number of Q_A (N) of NW-20% were the smallest, and the proportions of reaction centers (RCs) closed at 2 ms (V_J) and 30 ms (V_I) of N-20% were the highest. The increase in V_I for N-20% indicated the accumulation of reduced Q_A, which could not transfer electrons to the dark reactions (Pan *et al*. 2010). Thus, the activity of PSII in ES-20% was the highest. Our results demonstrated that chlorophyll *a* fluorescence can provided a relative accurate measure of PSII (Strasser *et al*. 2000; Strasser *et al*. 2004; Li *et al*. 2006).

NE-20%, NW-20%, and ES-20% had the highest Rg group content and Rg/Rb ratio. This result indicated that photooxidation occurred because Rg group are relatively weak antioxidants (Lü *et al*. 2012; Shkryl *et al*. 2018), whereas the highest value of P_n indicated that photooxidation did not affect P_n. In addition, the change in the total ginsenoside content was consistent with the change in P_n (Fig. 1A; Table 4), and the results agree with earlier works on *Panax Ginseng* L. (Jang *et al*. 2015).

Data suggested that E-W seedbed orientation was better for growing American ginseng than the N-S orientation for LTR of 20%. This is consistent with earlier works on other plants (Bai *et al*. 2005; Xu *et al*. 2011; Song 2017). For LTR of 15%, the total ginsenoside content, and the Rg and Rd groups were similar for both orientations and sides of the seedbeds.

The analysis of P_n, chlorophyll *a* fluorescence, and ginsenoside content showed that the lowest values were for E-11%, confirming that the lower light intensity was the sole limit source, subsequently affecting the ginsenoside contents (Xu *et al*. 2002). P_n and ginsenoside content increased with the LTR. According to the gas exchange parameters, the lowest P_n for LTR-11% was attributed to the stomatal factor.

Conclusion

The changes in the ginsenoside contents were consistent with the changes in LTRs and photosynthesis, whereas the lowest P_n at LTR of 11% was attributed to the stomatal factor. American ginseng plant grown on the E-W seedbeds with LTR of 20% had higher PSII activity and ginsenoside contents than the N-S seedbeds, regardless of the side of the seedbed. Moreover, the fluorescence data and ginsenoside contents showed that light oxidation occurred in PSII of plant leaves grown in the N-20% seedbed, even though the P_n was the highest. Therefore, future work should be focused on the long-term effect of light oxidation in American ginseng by prolonging the cultivation period for two or three years.

Acknowledgments

This study was supported financially by Shandong Province Modern Agricultural Industry Technical System via the Chinese Herbal Medicine Innovation Team Construction Project and the National Key Research and Development Project (2017YFC1702702, 2017YFC1700705).

References

Attele AS, JA Wu, CS Yuan (1999). Ginseng pharmacology: multiple constituents and multiple actions. *Biochem Pharmacol* 58:1685–1693

Bai YK, WH Liu, TL Wang, GH Tong (2005). Analysis of Orientation Influenced Sunlight in Solar Greenhouse. *Trans Chin Soc Agric Machin* 2:73–84

Campos Huitziméngari, C Trejo, CB Peña-Valdivia, R García-Nava, FV Conde-Martínez, R Cruz-Ortega MaDel (2014). Photosynthetic acclimation to drought stress in *Agave salmiana* Otto ex Salm-Dyck seedlings is largely dependent on thermal dissipation and enhanced electron flux to photosystem I. *Photosynth Res* 122:23–39

Bordenave CD, R Rocco, SJ Maiale, MP Campestre, OA Ruiz, AA Rodríguez, AB Menéndez (2019). Chlorophyll a fluorescence analysis reveals divergent photosystem II responses to saline, alkaline and saline–alkaline stresses in the two *Lotus japonicus* model ecotypes MG20 and Gifu-129. *Acta Physiol Plantarum* 41; Article 167

Cheng JF, YG Shen (2011). On the trends of photosynthesis research. *Chin Bull Bot* 46:694–704

Chinese Pharmacopoeia Commission (2015). *Pharmacopoeia of the People's Republic of China (First Part)*, pp:131–132. China Medical Science Press, Beijing, China

Cuchiara C, IM Silva, EG Martinazzo, EJ Braga, MA Bacarin, JA Peters (2013). Chlorophyll fluorescence transient analysis in *Alternanthera tenella* Colla plants grown in nutrient solution with different concentrations of copper. *J Agric Sci* 5:8–16

Force L, C Critchley, JJS van Rensen (2003). New fluorescence parameters for monitoring photosynthesis in plants. *Photosynth Res* 78:17–33

Hou LJ (2017). Cultivation and High-yielding cultivation techniques of American Ginseng in Weihai area. *Bull Agric Sci Technol* 7:283–286

Gao Y, W Liu, X Wang, L Yang, S Han, S Chen, RJ Strasser, BE Valverde, S Qiang (2018). Comparative phytotoxicity of usnic acid, salicylic acid, cinnamic acid and benzoic acid on photosynthetic apparatus of *Chlamydomonas reinhardtii*. *Plant Physiol Biochem* 128:1–12

Jang IB, DY Lee, Y Jin, HW Park, HS Mo, KC Park, DY Hyun, EH Lee, KH Kim, CS Oh (2015). Photosynthesis rates, growth, and ginsenoside contents of 2-yr-old *Panax ginseng* grown at different light transmission rates in a greenhouse. *J Ginseng Res* 39:345–353

Jedmowski C, A Ashoub, O momtazl, W Brüggemann (2015). Impact of drought, heat, and their combination on chlorophyll fluorescence and yield of wild barley (*Hordeum spontaneum*). *J Bot* 2015; Article 120868

Kim DH (2012). Chemical diversity of *Panax ginseng*, *Panax quinquefolium* and *Panax notoginseng*. *J Ginseng Res* 36:1–15

Kochan E, G Szymańska, P Szymczyk (2014). Effect of sugar concentration on ginsenoside biosynthesis in hairy root cultures of *Panax quinquefolium* cultivated in shake flasks and nutrient sprinkle bioreactor. *Acta Physiol Plantarum* 36:613–619

Li WL, ZH Wan, SY Yang (2014). Effects of different light transmission rate on American ginseng's photosynthesis. *Chin J Appl Ecol* 15;261–264

Li PM, HY Gao, RJ Strasser (2006). Application of the fast chlorophyll fluorescence induction dynamics analysis in photosynthesis study. *J Plant Physiol Mol Biol* 31:559–566

Liao B, H Newmark, R Zhou (2002). Neuroprotective effect of ginseng total saponin and ginsenosides Rb1 and Rg1 on spinal cord neurons in vitro. *Exp Neurol* 173:224–234

Liu TC, HQ Liu, RM Lv, BY Hu (1987). Dynamics of root growth and ginsenoside content of American Ginseng at different growth stages. *Chin J Chin Materia Med* 12:16–17

Lü JM, SM Weakley, Z Yang, M Hu, QZ Yao, CY Chen (2012). Ginsenoside Rb1 directly scavenges hydroxyl radical and hypochlorous acid. *Curr Pharm Des* 18:6339–6347

Ma J, C Lv, M Xu, PF Hao, YW Wang, WJ Shen, ZP Gao, GX Chen, CG Lv (2017). Analysis of chlorophyll a fluorescence and proteomic differences of rice leaves in response to photooxidation. *Acta Physiol Plantarum* 39; Article 46

Ma L, RN Wang, ZK Guo, S Zheng, X Zh, HN Liu, S Li, WR Xing, ZH Li, XY Zhang, Y Wang, LL Li, YH Li, Y Huang, Q Zhang, HR Wang (2015). Influence on Farmland Light Conditions of Crop Rows. *Mod Agric Sci Technol* 4:238–243

Pan X, D Zhang, X Chen, L Li, G Mu, L Li, W Song (2010). Sb uptake and photosynthesis of *Zea mays* growing in soil watered with Sb mine drainage: an OJIP chlorophyll fluorescence study. *Pol J Environ Stud* 19:981–987

Proctor JTA, JW Palmer, JM Follett (2010). Growth, dry matter partitioning and photosynthesis in North American Ginseng seedlings. *J Ginseng Res* 34:175–182

Proctor JTA, JW Palmer (2017). Optimal light for greenhouse culture of American ginseng seedlings. *J Ginseng Res* 41:370–372

Qi LW, CZ Wang, CS Yuan (2011). Ginsenosides from American ginseng: Chemical and pharmacological diversity. *Phytochemistry* 72:689–699

Qiu NW, F Zhou, ZJ Gu, SQ Jia, XA Wang (2012). Photosynthetic functions and chlorophyll fast fluorescence characteristics of five *Pinus* species. *Chin J Appl Ecol* 23:1181–1187

Rao MR, MC Palada, BN Becker (2004). Medicinal and aromatic plants in agroforestry systems. *Agrofor Syst* 61:107–122

Song W, C Li, X Sun, PZ Wang, SM Zhao (2017). Effects of ridge direction on growth and yield of tomato in solar greenhouse with diffuse film. *Trans Chin Soc Agric Eng* 33:242–248

Strasser RJ, A Srivastava, M Tsimilli-Michael (2000). The fluorescence transient as a tool to characterize and screen photosynthetic samples. *In: Probing Photosynthesis: Mechanism, Regulation and Adaptation*, Chapter 25, pp: 445–483. Yunus M, U Pathre, P Mohanty (eds). Taylor and Francis Press, London, UK

Strasser RJ, M Tsimill-Michael, Srivastava (2004). Analysis of the chlorophyll a fluorescence transient. *In: Advances in Photosynthesis and Respiration*, Chapter 12, pp:1–47. Gand P, Govindjee (eds). KAP Press, Dordrecht, The Netherlands

Stirbet A, Govindjee (2011). On the relation between the Kautsky effect (chlorophyll a fluorescence induction) and Photosystem II: Basics and applications of the OJIP fluorescence transient. *J Photochem Photobiol B Biol* 104:236–257

Sun S, LT Zhang, XH Yang, HY Gao (2009). Spectral reflectance and chlorophyll fluorescence kinetics of young leaves at the various stages of leaf expansion in field-grown chestnut plants. *Sci Silvae Sin* 45:162–166

Wang J, H Liu, WY Gao, LM Zhang (2013). Comparison of ginsenoside composition in native roots and cultured callus cells of *Panax quinquefolium* L. *Acta Physiol Plant* 35:1363–1366

Wang JH, WL Wu (2003). Study on the American ginseng's industrialization strategies in Huairou District in Beijing. *J Northwest Sci Technol Univ Agric For (Nat. Sci. Ed.)* 31:29–33

Wang SG, J Kong, SF Deng (2010). Cultivation techniques of American ginseng. *Mod Agric* 2:22–23

Xie JT, CZ Wang, M Ni, JA Wu, SR Mehendale, HH Aung, A Foo, CS Yuan (2007). American ginseng berry juice intake reduces blood glucose and body weight in ob/ob mice. *J Food Sci* 72:S590–S594

Xu AD, HC Xie, XQ Dai, C Yang, Y Wang, W Chen, HE Liu, XF Ye (2011). Effects of ridge-direction on photosynthetic characteistics of leaves in different positions in flue-cured tobacco field. *Acta Agric Jiangxi* 23:136–138

Xu KZ, ZH Wu, MS Zhan, MY Yang, ZA Zhang (2002). Temperature characteristics of photosynthesis of *Panax ginseng* and *Panax quinquefolius* leaves. *J Jilin Agric Univ* 24:7–10

Yu JP, XN Liu, JX Song, LM Li, YQ Zhang, J Zhou, CY Chen, SP Wang, Y Lin (2019). Comparison of ginsenosides from *Panax quinquefolium* L. by two different extraction methods. *J Binzhou Med Univ* 42:303–306

Yang C, DQ Zhang, MS Du, YH Shao, BT Fang, XD Li, JQ Yue, SY Zhang (2018). Effects of dark induced senescence on the function of photosystem II in flag leaves of winter wheat released in different years. *Chin J Appl Ecol* 29:2525–2531

Yuan CS, CZ Wang, SM Wicks, LW Qi (2010). Chemical and pharmacological studies of saponins with a focus on American ginseng. *J Ginseng Res* 34:160–167

Shkryl YN, GN Veremeychik, TV Avramenko, TV Avramenko, VV Makhankov, DV Bulgakov, YA Yugay, OL Burundukova, TI Muzarok, VP Bulgakov, YN Zhuravlev (2018). State of antioxidant systems and ginsenoside contents in the leaves of *Panax ginseng* in a natural habitat and an artificial plantation. *Acta Physiol Plantarum* 40; Article 124